Slice-based visualization of brain fiber bundles
A LIC-based approach

Stefan Philips[1], Mario Hlawitschka[2] and Gerik Scheuermann[1]
[1]*Leipzig University, Image and signal processing group, Germany*
[2]*Leipzig University of Applied Sciences, Faculty of computer science, mathematics and natural sciences, Germany*
{philips, scheuermann}@informatik.uni-leipzig.de, mario.hlawitschka@htwk-leipzig.de

Keywords: fiber bundles visualization, slice, MRI, dw-MRI, tractography, visualization, 2D

Abstract: The reconstruction of brain fibers from diffusion MRI data is a widely studied field. There is a great variety of algorithms to generate fiber tracts. Despite the many possibilities to create fiber tractograms, it is not very common within the medical community to make use of them. We think there are two reasons why the acceptance of this technique is so low. The first reason is that most time the degree of detail provided by singular fibers is neither justified nor needed. Second, within the medical domain tractography visualization is still uncommon. To solve the first problem it is common to apply clustering algorithms which aggregate the single fibers to fiber bundles. In this paper, we display the fiber bundles within slices. The presentation within slices is common within the medical community and very intuitive to examine. Furthermore, our visualization allows the spatial assignment of fiber bundles to the brain structure provided as T1 images. Among many neuroscientists and physicians, T1 images are the main source for spatial orientation within the brain.

1 INTRODUCTION

Diffusion-weighted magnetic resonance imaging (dw-MRI) is the only data source to reconstruct the neuronal connections of a living brain. A dw-MR image stores for each voxel the hydrogen diffusion profile. Brain fibers/axons are ensheathed by myelin, which is about 40 % water. Therefore the orientations of the axons influence the hydrogen diffusion profiles. Hence, it is possible to reconstruct nerve fibers from dw-MR images with tractography algorithms.

The dw-MR images are differentiated by their angular resolution. The most commonly used diffusion tensor images (DTI) with at least six measurements in different directions allows it to derive one main diffusion direction. The use of high angular resolution data imaging (HARDI) with more measurements in, e.g. 60, different directions makes it possible to compute a more realistic and detailed model of the diffusion profile per voxel. With the help of HARDI it is possible to extract several prominent diffusion directions per voxel.

The diffusion characteristic can be described by the diffusion orientation distribution function (ODF). The diffusion ODF is the marginal probability of diffusion in a given direction, which is computed for each voxel. Tuch 2004 introduced the diffusion ODF for dw-MRI. For our method, we use the improved variant of Aganj et al. 2010.

For a better comprehension of the remaining text we define the terms *brain fiber*, *fiber* and *fiber bundle*:

brain fiber: the actual biological

fiber: a trajectory reconstructed from the dw-MR data using a tractography algorithm

fiber bundle: a set of anatomically similar fibers

Especially the differentiation between a *brain fiber* and a *fiber*, which is reconstructed, is important. One has to be aware that a 7 T Scanner has a maximal voxel resolution of 1 mm edge length and a typical axon has a diameter of 1 µm. Considering this, ten thousands of axons can run through one voxel. With this in mind, one has to think of a reconstructed fiber as a representative for many real brain fibers. Since a reconstructed fiber is already a simplification, it makes sense for many use cases sense to reduce the data even more. This leads to the next logical step: the clustering of the reconstructed fibers by similarity. This clustering is done by fiber bundle algorithms, which typically use geometric shape and position of the fibers to measure similarity. The similarity, in turn, is used to group the fibers. These groups are the fiber bundles.

The awareness of the structural brain connectivity

should be very helpful for clinical and scientific appliances as well. But despite the fiber tractography algorithms are well explored, the acceptance within the medical community, especially in the clinical environment, is low.

[Hlawitschka et al., 2013] mentions the feedback from neuroscience experts for slice-based methods is very positive. The preference for slice-based visualizations among these experts has the following reasons:

- A simple but undeniable fact is the familiarity of neuroscientists and physicians with the slice-based data presentation. Slices allow them to explore and focus the data in a familiar way.
- Especially during the exploration of brain related data, the anatomical context is a very important asset. This can be achieved by combining a sparse slice visualization with anatomical image slices, e.g. T1 images.
- Slice-based techniques avoid occlusions.
- Medical documentation is often done in 2D.

Further Munzner 2014 gives a comprehensive overview of possible disadvantages resulting from 3D visualizations.

In this work, we introduce a visualization technique that has all the aforementioned advantages. Furthermore, our visualization works for difficult fiber configurations, like kissing or crossing fibers, and it can be used in combination with 3D fiber visualizations.

2 RELATED WORK

Our visualization approach relies on two kinds of preprocessing algorithms. It needs a fiber tracking and a fiber clustering algorithm.

There are a multitude of different fiber tracking algorithms. Behrens et al. 2014 give an overview of all three types of tractography algorithms. [Fillard et al., 2011] benchmarks different approaches. Probabilistic tractography algorithms are a special type of fiber tracking algorithm, which do not generate 3D trajectories as fibers. Briefly explained: Probabilistic tractography algorithms compute for each voxel of a dataset the connection likeliness to a seed voxels.

The trajectories of the aforementioned tractography algorithms can be clustered by a fiber clustering algorithm. Also for this task exists several algorithms.

The visualization of tractograms as 3D polylines is a competing and complementing approach to our technique as well. Therefore subsection 2.1 refers to work that displays fibers as 3D polylines.

In the last subsection, we present alternative slice-based dMRI-related visualization techniques. This overview of alternative techniques allows us to compare our method to them.

2.1 Visualization of 3D trajectories as polylines

The visualization of 3D trajectories has many applications and is therefore thematized by several publications which are not specifically related to reconstructed brain fibers, e.g. Zöckler et al. 1996 or Mallo et al. 2005.

Eichelbaum et al. 2013 addressed the problem of the spatial and the structural perception of reconstructed brain fibers to each other. With their LineAO approach, they contributed an algorithm to display fibers with better spatial and structural perception.

2.2 Slice-based visualization approaches

There already exist different approaches to visualize reconstructed brain fiber data in a slice based manner.

Goldau et al. 2011 introduced a technique to visualize probabilistic tractograms slice-wise. This approach was improved regarding the perception of tract probability by Hlawitschka et al. 2013. Lately Reichenbach et al. 2015b adapted the approach to HARDI data, that means they were able to illustrate possible kissing or crossing tracts of probabilistic tractograms.

Höller et al. 2012 proposed a slice-based technique which is based on a three-dimensional LIC. The necessary directions for the LIC is gained by extracting up to two maxima from the diffusion ODFs. The directions of the corresponding first maxima are used to apply a color coding to the LIC results. Höller et al. 2014 modify their slice visualization approach by replacing the input noise for the LIC algorithm with an image of diffusion glyphs.

Calamante et al. 2011 introduced track-density imaging (TDI). This technique counts the fibers crossing each voxel of a high resolution grid, allowing more insight into the white matter structure. Color coding can visualize the diffusion direction.

3 METHOD

In this section we introduce our slice-wise visualization of fiber bundles. In combination with a T1 image as an anatomical context, this allows a clear assignment of fiber bundles to the brain anatomy. These fiber bundles shall be distinguishable and traceable

within the slice. We start by explaining the necessary preprocessing steps – fiber tracking and fiber clustering. After that, we provide the detailed steps of our approach to achieve the aforementioned visualization. This includes:

- the creation of direction images for each bundle
- the creation of a noise texture, that allows the blending of the fiber bundle LIC-images
- the blending of the LIC-images

3.1 Preprocessing

The basic data input for our visualization method is a diffusion MRI dataset. Based on this data, our visualization method needs two preprocessing algorithms, the fiber tractography algorithm, and an algorithm to cluster the created fibers by similarity. The dependence of our processes is shown in Figure 1, where the preprocessing algorithms are marked yellow.

For both steps, tracking and clustering exist a bunch of algorithms. Behrens et al. 2014 give an overview of tractography algorithms and the work by Fillard et al. 2011 compares several fiber tracking algorithms. [Reichenbach et al., 2015a] compare their fiber clustering approach to four other techniques.

The preprocessing for our visualization starts with a given diffusion MRI dataset. This is used to create a fiber tractogram with a tracking algorithm. This tractogram is then clustered by a fiber clustering approach. The preprocessing data-flow is illustrated in Figure 1.

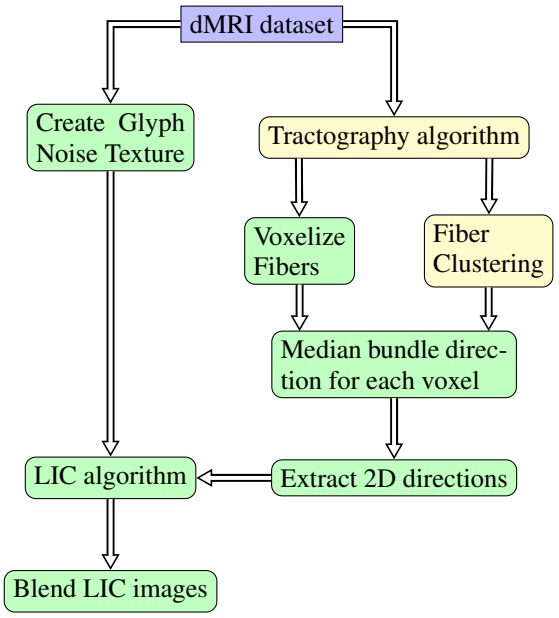

Figure 1: Data-flow during the processing. The colors purple, yellow or green mark if the boxes represent data, preprocessing or processing steps, respectively.

3.2 Processing

Once the preprocessing is done, three types of data are available for our visualization method. These are the dMRI dataset, the tractography and the clustering of the fibers. The process flow can be seen in Figure 1, where the actual visualization processes of our method are marked green.

The overall bundle-slice creation process of the bundle slices can be outlined the following four steps:

1. **Create 2D direction images**
   (a) **Voxelize Fibers:**
   calculate for each fiber which voxels it crosses
   (b) **Median bundle direction for each voxel:**
   calculate for each voxel the median direction from all fiber of a bundle
   (c) **Extract 2D-Directions:**
   create for each bundle per voxel the direction
2. **Create Glyph Noise Texture:**
   create a noise texture for the LIC algorithm using HARDI glyphs
3. **LIC algorithm:**
   compute a LIC image for each fiber bundle of the slice by using the 2D directions images from step 1 and the noise image from step 2
4. **Blend LIC images:**
   combine the different LIC images into one image

3.2.1 Create 2D directions image

Voxelize fibers

input: fiber tractography, fiber clustering

output: voxels with directions with annotated fiber cluster number

We calculate for each fiber which voxel it passes and store in each crossed voxel the local fiber direction. Currently, the resolution of the voxelized fibers is determined by the input dMRI dataset.

In detail the voxelization algorithm works as follow: The algorithm walks along the fiber points and processes two consecutive points after another. To determine which voxels are crossed by a fiber segment between two consecutive points $\mathbf{p}_i$ and $\mathbf{p}_j$, we use the rasterization algorithm Glassner [1990] which is based on the Bresenham algorithm 1965. The segment direction, annotated with the fiber cluster number of the currently processed fiber, is stored in every voxel that is determined by the aforementioned rasterization algorithm.

The result of this process are sets of directions $B_1, B_2, B_3, \ldots$ in each voxel. These sets group the directions, which are derived from the fibers, to the different fiber bundles.

Bundle median direction for each voxel

input: voxels with directions with annotated fiber cluster number

output: representative 3D direction for each fiber bundle for each crossed voxel

Now that we have the sets of directions $B_1, B_2, B_3, \ldots$ in each voxel with $B_i = \{\mathbf{d}_{i1}, \mathbf{d}_{i2}, \mathbf{d}_{i3}, \ldots\}$, we need to derive one representative direction for each set. Let B_i be one of these sets. We find the spatial median direction $\mathbf{d}_{i,\text{med}} \in B_i$ according to the following formula

$$\mathbf{d}_{i,\text{med}} = \underset{\mathbf{d} \in B_i}{\operatorname{argmin}} \sum_{j=1}^{n} \sphericalangle(\mathbf{d}_{ij}, \mathbf{d}), \tag{1}$$

where $\sphericalangle(\mathbf{a}, \mathbf{b})$ is the angle between the directions $\mathbf{a}$ and $\mathbf{b}$.

Extract 2D Directions

input: representative 3D direction for each fiber bundle for each crossed voxel

output: 2D vector images for each visualized bundle

For each fiber bundle, that crosses the current slice, a 2D vector image needs to be created. We obtain the 2D direction d^{2D} of the fiber bundle i by mapping the 3D direction $d^{3D} \in B_i$ to the slice plane. Given that our slices are aligned to the XY-, XZ- or YZ-plane, this can be done by taking the respective values of the 3D vector. For example the 3D direction $d^{3D} = (x, y, z)^T$ mapped to the XY-plane leads to $d^{2D} = (x, y)^T$.

3.2.2 Noise Image

The original LIC algorithm was proposed by Cabral and Leedom 1993 and uses two images as input: a 2D vector image and a noise image. The creation of the 2D vector image is described in the previous paragraph. Usually an image with white noise is as an input for the LIC-algorithm.

Glyph-based Noise Image

input: dMRI dataset

output: 2D gray scale image with glyphs

Höller et al. 2014 use samples of fiber-orientation-density (FOD) glyphs to generate a noise image for the LIC. The fiber orientations for the FOD glyphs are computed by using spherical deconvolution [Tournier et al., 2004] on the HARDI input. Then the glyph samples are placed along a path which results from a deterministic tracking within the slice.

For our visualization we use like Höller et al. 2014 a from glyphs generated noise image. For our goal to display clustered fibers within slices, we cannot use this a deterministic tracking algorithm. The deterministic tracking would most likely differ from the fibers to display and would be computational expensive.

Therefore we had to find a good placement scheme for the glyphs within the noise image. At a first glance the well-known glyph packing strategy by Kindlmann and Westin 2006 seems a suitable choice for the glyph placement problem, but it is designed for DTI Glyphs and would have to be extended for HARDI glyphs. Even if an extended variant would be available, it would be unnecessary complex for the actual task. In our case, the potential overlapping of some glyphs within the noise image is not problematic at all.

We tested three glyph placement strategies. The first one is a simple two-dimensional regular placement. The second variant distributes the glyphs uniform randomly within the slice. And the third variant uses Poisson-disk distribution to distribute the glyphs within the slice.

Points of a Poisson-disk distribution are randomly distributed and must be no closer than a specified value. To create this distribution we used the sampling algorithm proposed by Dunbar and Humphreys 2006. Our concrete implementation computes points within the 2D-range of $[0..1] \times [0..1]$. These coordinates are scaled to the full image size.

Figure 2 shows examples for the different glyph distributions. In Figure 2a one can see that the regular distribution pattern causes a regular pattern in the result image. The uniform random distribution causes a wild pattern in the resulting image, Figure 2b. The Poisson-disk distribution results in straight lines, Figure 2c.

The actual glyphs are created as follows: A icosahedron is tessellated with triangles to a certain degree. Then the normalized triangle vertex coordinates are used as input for the spherical harmonic function of the ODF. The resulting values describe the surface of the spherical function. This results in spherical harmonics glyphs like shown in Figure 3. The tessellation degree for these example glyphs is 2, which means each consists of 162 vertices. The coloring is done by using the absolute values of the normalized Euclidean direction as RGB color.

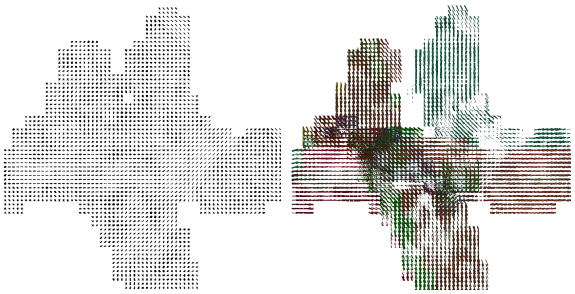

(a) Regular glyph distribution
Left: Noise image with regularly placed glyphs.
Right: The resulting visualization for regulary placed glyphs.

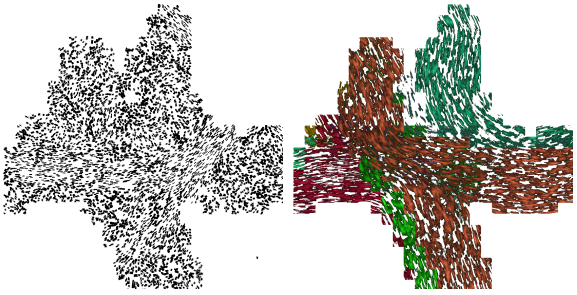

(b) Uniform random glyph distribution
Left: Noise image with uniform randomly placed glyphs.
Right: The resulting visualization for uniform randomly placed glyphs.

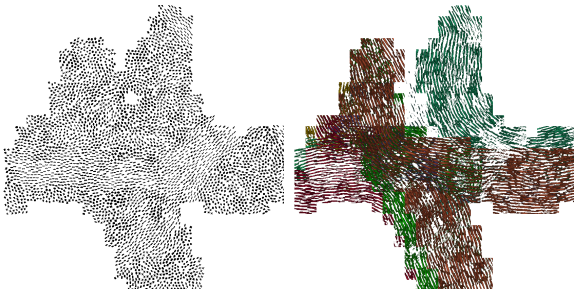

(c) Poisson-disk glyph distribution
Left: Noise image with Poisson-disk distributed glyphs.
Right: The resulting visualization for Poisson-disk distributed glyphs.

Figure 2: Different glyph distributions and the corresponding result of the algorithm

3.2.3 Special case: Orthogonal bundles

Fiber bundles which run orthogonal or almost orthogonal to the displayed slice would not be visualized in a reasonable way by the LIC-method. This results from the fact that there is not enough directional information for this bundles within the slice.

Therefore we determine the orthogonal bundles and display them by coloring their slice area with their transparent cluster color (alpha value 0.5). Which fiber bundles are considered to be orthogonal bundles

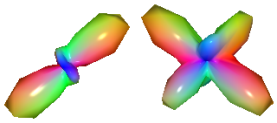

Figure 3: Spherical harmonics glyphs composited from 162 vertices. The absolute values of the Euclidean direction vectors are used as RGB color vector (RGB coloring).

is determined by the percentage of the average bundle direction-vector-component that is orthogonal to the current slice.

3.2.4 LIC process and Coloring

input: direction image for each bundle that crosses the current slice and the glyph noise image

output: a LIC image for each bundle that crosses that crosses the current slice

The LIC implementation is the original algorithm like it was proposed by Cabral and Leedom 1993, but of course it uses the adapted noise image. The coloring is done bundle-wise, apart from that the actual color of each fiber bundle can be arbitrary selected. For example one can use RGB direction coloring, selection coloring or any other bundle-wise coloring.

3.2.5 Blending the Bundle Layers

input: a LIC image for each bundle that crosses the current slice

output: final slice

After the LIC algorithm is done for every bundle. It is necessary to merge the output of all LIC processes into one image. This is done by drawing one LIC image after another into the space left by the previous LIC images. A pixel with RGB color $\mathbf{c}$ is considered free if $\|\mathbf{c}\|_{\max} < 0.2$ is true. The blending order is determined by the size of the bundles within the slice. The blending process starts with the LIC image of the smallest bundle. This should ensure the maximum visibility of the fiber bundles in the slice.

4 RESULTS

We tested our visualization with two datasets. The first one is the synthetic Fiber Cup phantom dataset [Fillard et al., 2011]. The Fiber Cup dataset is a dw-MRI scan of a hardware phantom. It was originally created to test tractography algorithms. We choose this one because of its clear structure and the

Table 1: Properties of the datasets to test the visualization.

Dataset	Fiber Cup	Human brain
voxel size (mm^3)	$3 \times 3 \times 3$	$1.7 \times 1.7 \times 1.7$
dimensions	$64 \times 64 \times 3$	$128 \times 128 \times 72$
diffusion directions	128	60

known ground truth. It has typical difficult fiber bundle configurations like kissing, crossing and spreading fiber bundles. The second one is a dw-MR image of a healthy human brain. It was acquired with a 3 T Siemens Trio MRI scanner using single echo spin echo Echo-Planar Imaging (EPI) sequence with GRAPPA on a 32 channel coil. Table 1 shows the image properties of both datasets.

4.1 Fiber Cup dataset

Figure 4a shows the whole dataset using our visualization. The planar shape and the different fiber bundle configurations make the Fiber Cup dataset ideal to demonstrate slice based visualization approaches. Since we know the ground truth of the Fiber Cup dataset we reduced it by removing identified outliers to 250 fibers. The fibers were generated with the streamline tractography algorithm by Lazar et al. 2003 using the implementation from tensor toolkit 1.4 [1]. Except for $FA_1 = 0.2$ and $FA_2 = 0.3$ we used the default parameter. We used the QuickBundles [Garyfallidis et al., 2012] algorithm to cluster the tractograms. Heuristically we determined the parameter $\theta = 225$ to get a clustering close to the known ground truth of 7 fiber bundles.

For the visualization example in Figure 4a we used a Poisson-disk radius of 0.0045, a glyph size of 0.4 and 30 LIC steps at maximum. The separate fiber bundles are clearly identifiable and the course at crossings is also traceable. The close-ups of crossings in Figure 4b and 4c show that the bundles are clearly differentiable The image shows also a disadvantage of the current implementation: Due to the low resolution of the voxelized fibers, the displayed fiber bundles overlap the white matter. The low resolution is also the reason for the raw block shape of the displayed fibers.

4.2 Human brain dataset

The dataset of a healthy human brain allows us to show a real world example. Figure 5a visualizes a frontal view of a coronal slice. We used the deterministic spherical-deconvolution (SD) [Tournier et al., 2004] based fiber tracking algorithm from MRtrix[2] with its default parameters. The clustering was done with the approach by Reichenbach et al. 2015a. For the visualization, we used the same parameter as before, a Poisson-disk radius of 0.0045, a glyph size of 0.4 and 30 LIC steps at maximum. We selected a slice where the corticospinal tracts (CST, blue) and the corpus callosum (CC, red) cross. The detail views of the crossings in the left and right hemisphere are shown in Figure 5c and 5b, respectively. The corticospinal tract is traceable crossing the corpus callosum.

Figure 6 shows the LineAO approach by Eichelbaum et al. 2013 and our slice-based visualization combined. To select the displayed 3D trajectories, we used a Region-of-Interest (ROI) box. By using this combination, the user can benefit from the advantages of 2D and 3D visualization. Whereas the 3D trajectories provide a good overview, the strength of

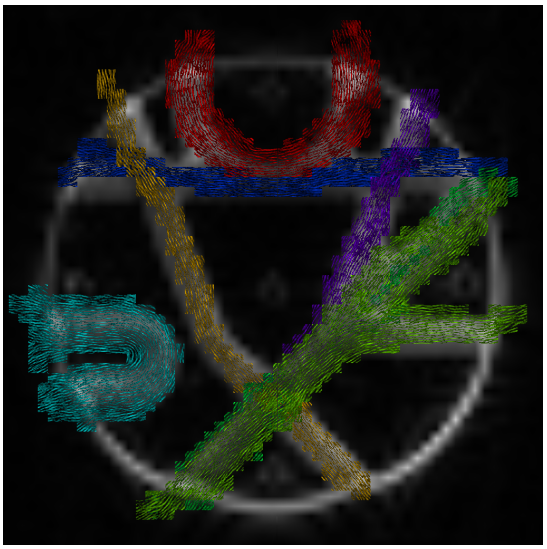

(a) Visualization for the fibercup dataset bundles.

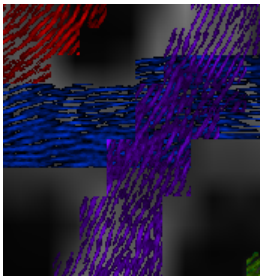

(b) Detail of the crossing in the upper-right area.

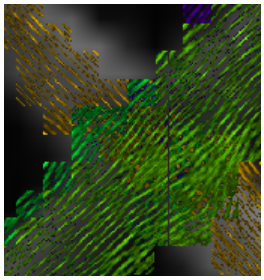

(c) Detail of the crossing in the bottom-middle area.

Figure 4: The presented algorithm applied to the Fiber Cup dataset, including three detail views.

[1] https://gforge.inria.fr/projects/ttk

[2] http://jdtournier.github.io/mrtrix-0.2/tractography/tracking.html

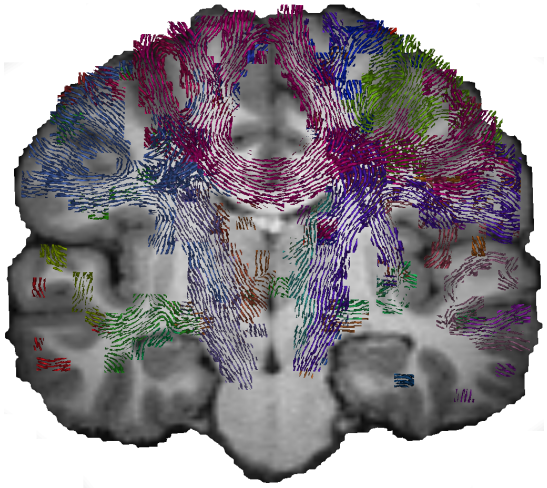

(a) Visualization for a coronal slice. Showing among other fiber bundles the corpus callossum (CC, red) and the cortico spinal tract (CST, blue.)

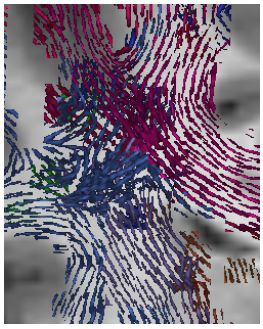

(b) Crossing of CC (red) and CST (blue) in the right hemisphere.

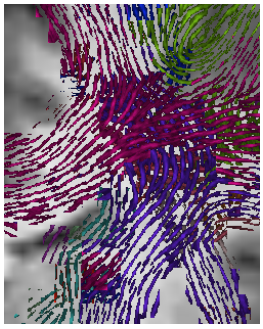

(c) Crossing of CC (red) and CST (blue) in the left hemisphere.

Figure 5: Visualization of Coronal slice and two detail views. Orthogonal fiber bundles are suppressed.

our approach is the fast view into spatial details, without using a ROI box and the clear perception of the anatomical context, represented as T1 image.

4.3 Comparison to existing visualizations

Depending on the application the presented method has advantages over the previously mentioned visualization approaches.

In contrast to 3D polylines, a slice based fiber bundle visualization allows the easy assignment to an anatomical context by using T1 images. Besides the slice-wise view to medical data is well-established. Given that slice-based methods are two-dimensional, they are suitable for clinical documentation purposes.

The advantage of the presented method over the approach by Höller et al. 2014 is the use of reconstructed tractograms. Höller et al. 2014 perform an own tracking for their visualization. This tracking is reduced to the currently displayed slice. Because of this locality, it does not cover the complex task of fiber reconstruction from diffusion MRI data. The comparison of fiber tractography algorithms by Fillard et al. 2011 suggests that especially the use of global information is advisable. The presented method can use many available fiber tractography algorithms. The information complexity of the reconstructed fiber configurations is further decreased by the use of a fiber bundle algorithm.

The method by Reichenbach et al. 2015b is specialized for probabilistic tractograms. The adaptation to general fiber tractograms would be possible, but the visualization of deterministic fiber tractograms in a glyph-based manner is counter-intuitive and increases unnecessarily the visual complexity.

The aforementioned TDI approach [Calamante et al., 2011] generates a super-resolution T1-like image from a tractogram. TDI does not aim to visualize concrete fibers or fiber bundles.

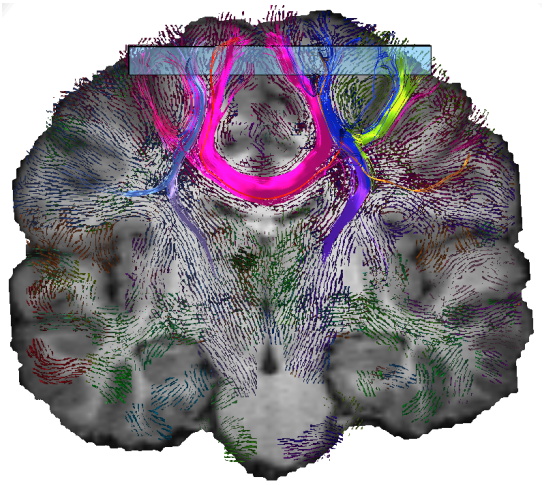

Figure 6: The combination of 3D streamline and slice-based visualization.

5 SUMMARY

We presented a new visualization approach that allows a slice-wise examination of fiber bundles. This slice-wise inspection has several useful properties and is intended as a supplement to conventional 3D trajectory visualization of fiber bundles. The combination of this visualization techniques is shown in Figure 6.

Further, the slice-wise presentation allows a clear assignment of the fiber bundles to the structural infor-

mation provided by a T1 image. Many neuroscientists use the structural information provided by a T1 image as spatial orientation. The familiarity of medical staff with slice-based data can also be considered as an advantage of the method. Furthermore, a 2D visualization is well suited for medical documentation. Another inherent advantage of a 2D approach is the avoidance of occlusion.

We have shown that the visualization works also for difficult fiber bundle configurations like crossings, see the Figures 5b, 5c, 4b, and 4c. The visibility of the relation between the fiber bundles and anatomy is a strength of the visualization method, too. The Figures 4a and 5a allow it to relate the fiber bundle to structural information given by T1 image.

REFERENCES

Aganj, I., Lenglet, C., Sapiro, G., Yacoub, E., Ugurbil, K. and Harel, N. (2010). Reconstruction of the orientation distribution function in single-and multiple-shell q-ball imaging within constant solid angle. Magnetic Resonance in Medicine *64*, 554–566.

Behrens, T. E., Sotiropoulos, S. N. and Jbabdi, S. (2014). MR Diffusion Tractography. In Diffusion MRI - Second Edition, (Johansen-Berg, H. and Behrens, T. E., eds), chapter 19, pp. 429–451. Elsevier Inc. London.

Bresenham, J. E. (1965). Algorithm for computer control of a digital plotter. IBM Systems journal *4*, 25–30.

Cabral, B. and Leedom, L. C. (1993). Imaging Vector Fields Using Line Integral Convolution. In Proceedings of the 20th Annual Conference on Computer Graphics and Interactive Techniques SIGGRAPH '93 pp. 263–270, ACM, New York, NY, USA.

Calamante, F., Tournier, J.-D., Heidemann, R. M., Anwander, A., Jackson, G. D. and Connelly, A. (2011). Track density imaging (TDI): validation of super resolution property. Neuroimage *56*, 1259–1266.

Dunbar, D. and Humphreys, G. (2006). A Spatial Data Structure for Fast Poisson-disk Sample Generation. In ACM SIGGRAPH 2006 Papers SIGGRAPH '06 pp. 503–508, ACM, New York, NY, USA.

Eichelbaum, S., Hlawitschka, M. and Scheuermann, G. (2013). LineAO — Improved Three-Dimensional Line Rendering. IEEE TVCG *19*, 433–445.

Fillard, P., Descoteaux, M., Goh, A., Gouttard, S., Jeurissen, B., Malcolm, J., Ramirez-Manzanares, A., Reisert, M., Sakaie, K., Tensaouti, F., Yo, T., Mangin, J.-F. and Poupon, C. (2011). Quantitative evaluation of 10 tractography algorithms on a realistic diffusion MR phantom. NeuroImage *56*, 220 – 234.

Garyfallidis, E., Brett, M., Correia, M. M., Williams, G. B. and Nimmo-Smith, I. (2012). Quickbundles, a method for tractography simplification. Frontiers in neuroscience *6*, 175.

Glassner, A. (1990). Graphics Gems I.

Goldau, M., Wiebel, A., Gorbach, N. S., Melzer, C., Hlawitschka, M., Scheuermann, G. and Tittgemeyer, M. (2011). Fiber Stippling: An Illustrative Rendering for Probabilistic Diffusion Tractography. In IEEE BioVis Proceedings pp. 23–30, IEEE.

Hlawitschka, M., Goldau, M., Wiebel, A., Heine, C. and Scheuermann, G. (2013). Hierarchical Poisson-Disk Sampling for Fiber Stipples. In 3rd Intl. Workshop on VMLS pp. 19–23, Eurographics, Leipzig.

Höller, M., Otto, K. M., Klose, U., Groeschel, S. and Ehricke, H. H. (2014). Fiber Visualization with LIC Maps Using Multidirectional Anisotropic Glyph Samples. Journal of Biomedical Imaging *2014*, 9:9–9:9.

Höller, M., Thiel, F., Otto, K.-M., Klose, U., Ehricke, H.-H. and Schwedenschnaze, Z. (2012). Visualization of High Angular Resolution Diffusion MRI Data with Color-Coded LIC-Maps. In GI-Jahrestagung pp. 1112–1124, GI.

Kindlmann, G. and Westin, C.-F. (2006). Diffusion tensor visualization with glyph packing. IEEE Transactions on Visualization and Computer Graphics *12*.

Lazar, M., Weinstein, D. M., Tsuruda, J. S., Hasan, K. M., Arfanakis, K., Meyerand, M. E., Badie, B., Rowley, H. A., Haughton, V., Field, A. et al. (2003). White matter tractography using diffusion tensor deflection. Human brain mapping *18*, 306–321.

Mallo, O., Peikert, R., Sigg, C. and Sadlo, F. (2005). Illuminated lines revisited. In VIS 05. IEEE Visualization, 2005. pp. 19–26, IEEE.

Munzner, T. (2014). Visualization analysis and design. CRC press.

Reichenbach, A., Goldau, M., Heine, C. and Hlawitschka, M. (2015a). V-Bundles: Clustering Fiber Trajectories from Diffusion MRI in Linear Time. In MICCAI (1), (Navab, N., Hornegger, J., III, W. M. W. and Frangi, A. F., eds), vol. 9349, of LNCS pp. 191–198, Springer.

Reichenbach, A., Goldau, M. and Hlawitschka, M. (2015b). Fiber Stipples for Crossing Tracts in Probabilistic Tractography. In Proc. of VCMB '15 pp. 113–122, EG.

Tournier, J.-D., Calamante, F., Gadian, D. G. and Connelly, A. (2004). Direct estimation of the fiber orientation density function from diffusion-weighted MRI data using spherical deconvolution. NeuroImage *23*, 1176–1185.

Tuch, D. S. (2004). Q-ball imaging. Magnetic resonance in medicine *52*, 1358–1372.

Zockler, M., Stalling, D. and Hege, H.-C. (1996). Interactive visualization of 3D-vector fields using illuminated stream lines. In Visualization'96. Proc. pp. 107–113, IEEE.